Absolute measurement of the photoionization cross section of atomic hydrogen with a shock tube for the extreme ultraviolet

H. P. Palenius, J. L. Kohl, and W. H. Parkinson
Center for Astrophysics, Harvard College Observatory, and Smithsonian Astrophysical Observatory, Cambridge, Massachusetts 02138
(Received 13 August 1975)

The photoionization cross section of H I was measured at 19 wavelength points from 910 to 609 Å with experimental uncertainties between 7 and 20%. An aerodynamic shock tube, equipped with explosively driven shutters, was used to produce fully dissociated hydrogen and neon gas mixtures for the photoabsorption measurements. A description of the new shock-tube facility and a discussion of the experimental techniques are presented. Since our results agree with well-established theory, the reliability of our apparatus and methods for making measurements of this kind has been demonstrated. The measurement is the first in a continuing program to measure the photoionization cross sections of H I, O I, C I, and N I.

I. INTRODUCTION

The experiment reported in this paper is part of a program to measure the absolute values of the atomic photoionization cross sections of astrophysically abundant elements. Atomic photoionization cross sections are necessary for model calculations of the emergent intensity of stars[1] and are also used in the studies of the heating mechanisms and the chemistry of planetary atmospheres.[2,3]

The previous absolute measurements of atomic photoionization in this laboratory[4-8] were limited to wavelength regions above the transmission limit of LiF, which has the shortest wavelength limit of any material that is suitable for shock-tube windows. In order to measure the photoionization cross sections of H I, C I, N I, and O I, it has been necessary to extend our measurement capability to the wavelength region around and below this limit. Therefore an aerodynamic shock tube was equipped with explosively driven shutters that are capable of creating an open optical path through a shock-heated gas in a few μsec. Our initial results with this new facility are the first measurements of the photoionization cross section of atomic hydrogen near the series limit (λ911 Å) and also of the variation of the cross section with wavelength down to 600 Å. Because our results agree with well-established theory,[9,10] these measurements confirm the reliability of our apparatus and our technique for making measurements of this kind. Previously, this cross section had been measured[11,12] at three wavelength points (850.6, 840.0, and 826.3 Å).

The experimental values for the H I photoionization cross section reported here were determined with absorption spectrometry measurements of hot neon and hydrogen gas mixtures behind reflected shock fronts in a pressure-driven shock tube. Shock-heated gases are well suited to absolute absorption measurements because they have well-defined and measurable thermodynamic properties, they are very homogeneous, and the atomic density is high enough for photoionization measurements. The conditions for a very high degree of dissociation of the molecules can often be achieved, as they were in this case.

II. EXPERIMENTAL ARRANGEMENTS

A. Shock tube

All measurements were made with an aerodynamic pressure-driven shock tube (shown schematically in Fig. 1) constructed from stainless steel with a quadratic cross section with sides of 5.12 $\pm$0.01 cm. The driver section was separated from the 7.4-m-long channel and test section by an aluminum (type 1100) diaphragm of 0.8 mm thickness. The diaphragms were stamped with X-shaped marks in order to achieve a fairly consistent rupture pressure. Hydrogen at about 45 atm served as the driver gas and the diaphragms ruptured by an overpressure in the driver section.

The test-gas mixture of (0.5–1)% H_2 in Ne was prepared in a gas-handling system that was evacuated to better than 1×10^{-5} Torr prior to making the mixture. The hydrogen quantity was measured with a MKS Instruments Baratron capacitive diaphragm bridge manometer; after the neon was added, the total pressure was measured with a Wallace and Tiernan model FA145 precision dial manometer. Large gas quantities were used in order to achieve accurate mixtures, and a new mixture was prepared before each shock. The total initial test-section pressure was varied between 5 and 7 Torr. The pressure rise in the shock tube after the pump valve was closed did

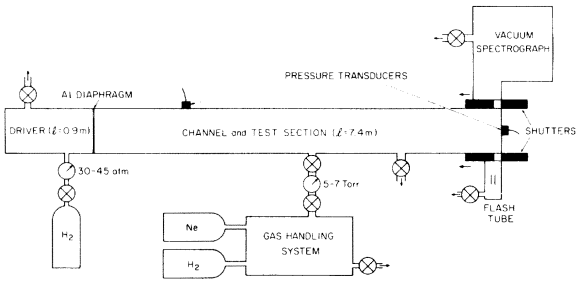

FIG. 1. Schematic diagram of the experimental arrangement.

not exceed 4×10^{-4} Torr before the measurements were made. Two Kistler pressure transducers were used. One of them (model 601A) was placed 1.6 m from the diaphragm in the channel section. The other pressure transducer (model 201B) was placed in the end-plug wall very near the test area.

B. Shutter mechanism

A pair of close-open-close shutters were used to create an open light path through the shock-heated gas during the period of the measurement. A similar shock tube having one shutter was previously described by Marrone and Wurster.[13]

Our shutter mechanism is shown schematically in Fig. 2. The openings in the shock-tube wall had rectangular cross sections of 1×3 mm and were placed so that the light path from the flashlamp to the spectrograph passed diagonally through the quadratic cross section of the shock tube and perpendicular to its long dimension. The shock-tube wall thickness at the openings was 0.7 mm. The openings in the shutters were pre-evacuated.

After the ignition of the explosive charge (squib) in the combustion chamber, the piston drove the yoke and both shutters so that they opened and closed simultaneously. The squibs were supplied by ICI United States, Inc. The shutters were accelerated to a speed of 61 $msec^{-1}$. It took 1525 ± 25 μsec from the time the squib was triggered until the shutters opened. The shock absorbers that were used to stop the shutters consisted of brass tubes that were deformed during deceleration by oversized plungers. The aluminum shutters contacted their shock absorbers about 380 μsec after the piston had contacted its shock absorber. The brass tubes had to be replaced after each firing. The piston and the shutters have not been replaced after 60 firings.

A light signal through the yoke aperture was used to start the electronics for the coaxial flashlamp and the lamps for the temperature measurements, as described in Sec. II F.

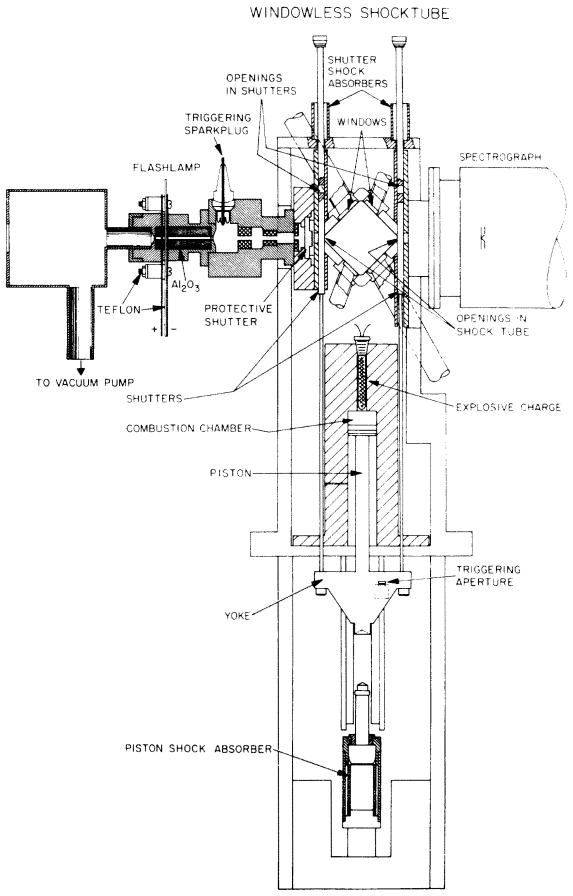

FIG. 2. Cross-sectional view of the shock tube showing the shutter mechanism and the flashlamp.

Gas will flow through the openings in the shock-tube walls when the shutters open. The amount of gas flowing into the flashlamp volume was measured by keeping the pump valve closed during a shock experiment. The measured number density of particles flowing through the opening was found to be of a value between values calculated from equations of molecular flow[14] and of critical flow[15] through orifices. An upper limit of about 4% absorption in addition to the absorption of the gas within the shock tube was determined as the total effect of this gas flow.

C. Absorption apparatus

The optical arrangements are shown schematically in Fig. 3. Three optical axes were used. The axes were coplanar and at a distance of 18.4 mm from the end-plug wall. The optical path containing the shutters was used for the absorption measurements. The spectrograph was a 1-m McPherson model equipped with a Bausch

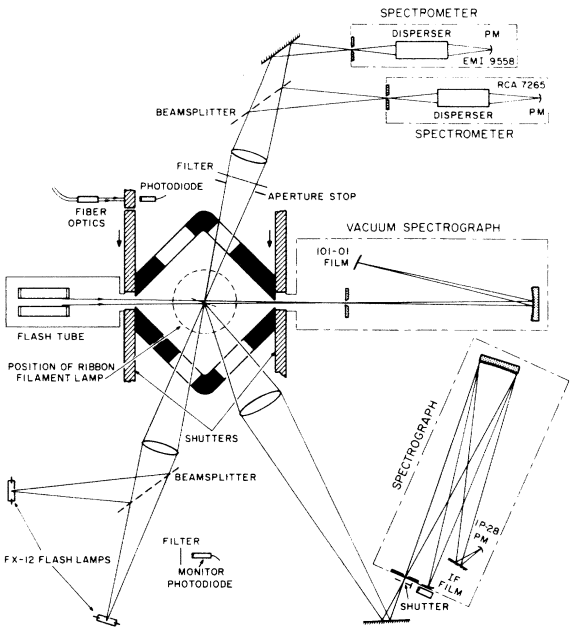

FIG. 3. Schematic diagram of the optical arrangements for the absorption measurements, the brightness-emissitivy temperature measurements, and the determination of the visible spectrum.

and Lomb gold-coated grating blazed at 1200 Å. Slit widths from 40 to 250 μm were used.

A modified Garton-type[16] coaxial flashlamp (see Fig. 2) was used to produce an intensive background continuum of about 2-μsec duration. A 15-μF capacitor charged to 10 kV was discharged through an Al_2O_3 tube of 5 cm length and 2 cm outer diameter. A 3-mm bore was chosen so that the discharge was concentrated within the optical field of the absorption apparatus. The flash tube was kept evacuated at a pressure of about 1×10^{-2} Torr and a system of apertures between the flashlamp and the shock tube were used to prevent the discharge from reaching the shock tube. The flash-to-flash variation in intensity was found to be $\pm5\%$.

The intensity of the flash-tube continuum varied slowly with wavelength and was useful down to about 500 Å, where the spectrum becomes dominated by emission lines. In the wavelength region used for the photoabsorption measurements (1200–600 Å) the background continuum showed some absorption lines of ionized oxygen and aluminum.

The absorption spectra were recorded on Kodak 101-01 film. Each film was calibrated with a set of intensity exposures from one flash of the background lamp through mesh filters of measured transmission that were placed in the light path inside the evacuated shock tube. The films were presoaked in distilled water for 3 min and developed for 5 min in Kodak D-19 developer, diluted 1:2, at 20°C.

A characteristic curve for the wavelength of each photoabsorption data point was constructed for each film. The consistency in the shapes of the characteristic curves for various films is shown in Fig. 4. The data points of the calibration exposures from each of ten films at two wavelengths, 910 and 635 Å, are plotted. All points from the same film are designated with symbols of the same shape. In order to adjust for differences in the light flux at the film due to changes in the exposure conditions, all points from each film at a given wavelength have been shifted by the same distance along the logarithmic scale of the abscissa. The transmission scale of Fig. 4 was set by the characteristic curve of the film with the highest densities at λ910 Å. The transmissions through the shock-heated gas were almost always determined from the linear part of the individual characteristic curves.

D. Temperature measurement apparatus

One of the other optical axes (see Fig. 3) was used for determining the temperature of the shock-heated gas with the brightness-emissivity method.[17] The emissivity of the gas was determined by measuring the transmittance through the shock-heated gas of the radiation produced by an FX-12 xenon flashlamp (E.G. & G., Inc.). Sometimes the light from a second FX-12 lamp was brought into the optical path through the shock tube with a beam splitter in order to check that the temperature stayed constant throughout the time period of the measurements. The intensity of the FX-12 lamp was monitored with a photodiode and an optical interference filter.

Two Jarrell-Ash 0.5-m spectrometers were used in the first order, one set at the λ6562-Å HI line (Hα) and the other at the λ6402-Å NeI line. An absorption filter was placed in the optical path to block higher diffraction orders. An RCA 7265 and an EMI 9558 photomultiplier were used to detect the shock-emitted intensity and the FX-12 light. The linearity of the photomultipliers was checked with neutral-density filters for the current region used, which extended over nearly three orders of magnitude. The shock emission was compared with the intensity of the center of a transfer General Electric tungsten ribbon lamp, which was placed in the shock tube. The lamp was used to transfer the calibration of a Philips standard of spectral radiance into the shock tube.[18]

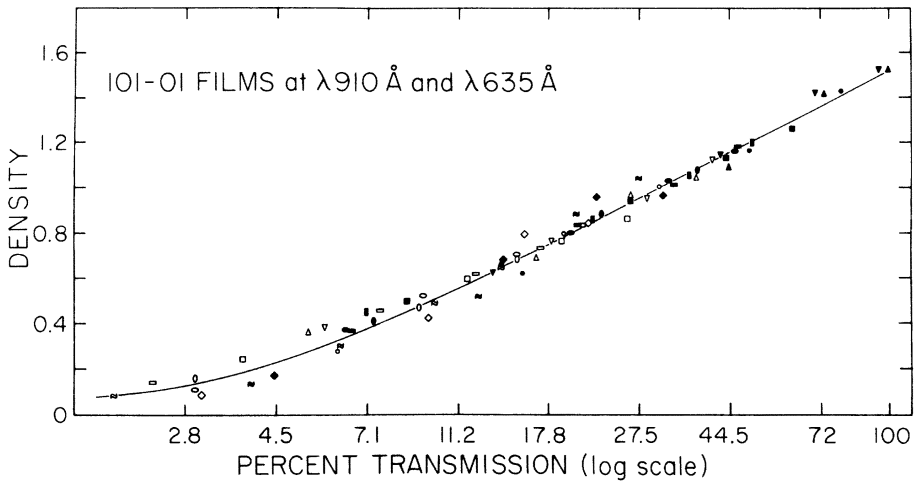

FIG. 4. Comparison of the characteristic curves for ten films for λ910 Å (solid symbols) and λ635 Å (open symbols).

E. Visible spectrum apparatus

The third axis (also shown in Fig. 3) was used to record photographically the visible emission spectrum of the shock-heated gas with a Bausch and Lomb 1.5-m spectrograph on Kodak IF or high-speed infrared film. An exploding-wire-driven shutter[19] placed close to and in front of the entrance slit was used to obtain a time-resolved spectrum and the opening and closing of this blast shutter was monitored photoelectrically at the zero-order image.

F. Electronic system

A block diagram of the electronic system is shown in Fig. 5, together with a time axis indicating typical times of events during a shock. The electronics were divided into three sections that were independently triggered at times which depended on the shock speed and the speed of the shutters. The arrival of the shock front at the channel section and end-plug pressure transducers provided pulses, which after amplifications and delays were used to trigger, respectively, the

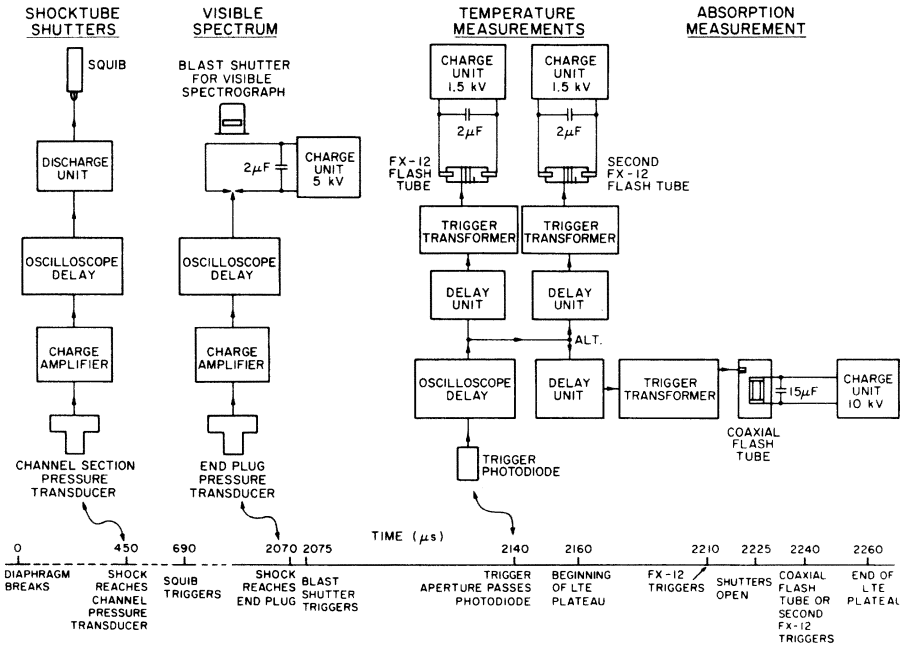

FIG. 5. Top: Block diagram of the electronics. Bottom: Timing sequence for the shock events.

shutters for the absorption measurement and the shutter for the 1.5-m spectrograph. The aperture in the yoke passed the photodiode (see Figs. 2 and 3) about 75 μsec before the shock-tube shutters were fully open. The signal from the photodiode, after delays in two different circuits, was used to trigger the lamps for the temperature and the photoabsorption measurements. The delays were preset so that the shutters opened and the lamps fired during the time when the shock-heated gas was in equilibrium.

The signals from the three photomultiplier tubes, the two photodiodes, and the two pressure transducers were recorded on Tektronix 555 dual-beam oscilloscopes.

III. THE MEASUREMENTS

A. Shock-heated gas

Figure 6(a) gives oscilloscope traces of the outputs of the end-plug pressure transducer (A and D), the NeI (6402 Å) detector (B), and the Hα detector (C) for a typical shock. Trace A begins when the shock front reaches the channel section transducer, and has a sweep rate of 200 μsec per division. The Mach number of the shock is determined from this trace. Traces B, C, and D are delayed with respect to A by 1505 μsec, and have sweep rates of 50 μsec per division. The numbers in Fig. 6 refer to traces B, C, and D, and correspond to events that are partially listed in Fig. 5.

At time 1 the incoming shock front reaches the end plug, at time 2 the reflected shock front passes the optical axis of the temperature-measurement apparatus, and the emission from the heated gas at the wavelength of Hα will be seen by the photomultiplier tube. During the period of about 40 μsec until point 3, the gas is far from local thermodynamic equilibrium (LTE) conditions. The Hα intensity and the pressure are slightly increasing. The Hα line is narrow and not Stark broadened, which indicates that the electron number density is low and that there are too few electrons to reach LTE conditions at the $n=3$ level in HI. The apparent temperature measured by the brightness-emissivity method at Hα is 6500 K. Between points 3 and 4 the intensity of Hα increases and the pressure becomes constant. We would expect dissociation to be completed during this period and that excitation, ionization, and electron production take place. The many electrons produced distribute the energy and the hot gas is brought into LTE. Between points 4 and 5, the LTE plateau, the pressure is constant, and the emission intensity both from Hα and the NeI λ6402-Å line are constant.

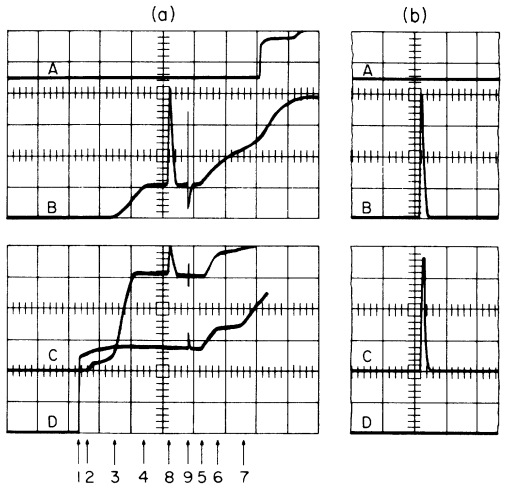

FIG. 6. Oscilloscope traces of the signals from the end-plug pressure transducer (A and D), the photomultiplier signals at the wavelength for the Ne I 6402-Å line (B), and the Hα line (C), (a) during a shock, and (b) without a shock. Events at the numbers are explained in the text.

At point 5 of Fig. 6 the shock front arrives a second time at the test section, after being reflected at the contact surface.[20] The emission intensity is raised to a second plateau between points 6 and 7, with an apparent temperature of about 16 500 K. At point 9 the electronic pickup signal indicates the time when the flash tube for the absorption measurements was fired.

B. Temperature

The temperature of the shock-heated gas was determined by the brightness emissivity method[17] using the Hα line and also using the λ6402.25-Å NeI line. This method provides a measurement that is independent of any knowledge of atomic parameters.

The traces of Fig. 6(b) correspond to those of Fig. 6(a) for a test run with no shock. The pulse trace for the light from the FX-12 lamp can be seen on these traces. For the temperature measurements, the emissivity was determined from the ratio between the pulse height above the emission of the shock-heated gas [Fig. 6(a), point 8] and the pulse height obtained by flashing the FX-12 lamp through the evacuated shock tube [Fig. 6(b)]. Over the course of the experiment, different portions of the Hα line were used for the measurements. The values of emissivity were determined to be within the range 0.3–0.8.

The measured temperatures determined from Hα and the 6402.25-Å NeI line were found to be equal to within ±2%. The temperature remained constant between points 4 and 5 of Fig. 6(a). The

lower and upper excitation potentials of Hα are 10.2 and 12.09 eV, respectively. The excitation potentials of the 6402.25-Å NeI line (16.63 and 18.56 eV) are larger then the ionization potential of atomic hydrogen. The fact that the excitation temperatures of the NeI line and Hα are in agreement is a strong indication that the assumption of LTE is valid.[21]

C. Electron number density

The chemical equilibrium calculation (see Sec. IV A) provides a value for the electron number density. We made an independent check of these results by determing the electron density from the Hβ line profile.[22,23] This line is dominatly Stark broadened. Doppler broadening, instrumental broadening, other broadening effects,[24] and self-absorption were known to be minor and were therefore neglected. The asymmetry of the two halves of the profile was averaged. Although we have only a limited amount of data, the measured electron density agreed with the chemical equilibrium value.

The collisional processes must maintain the LTE population distribution during the period of the measurements. The minimum electron number density necessary to give LTE for a given energy level is, according to Griem,[25]

$$N_e \geq 1\times 10^{11} Z^7 T^{1/2} (\Delta E)^3, \qquad (1)$$

where T is in K, ΔE in eV, and N_e in cm^{-3}. The equation is believed to hold for the case where the gas is optically thick for the resonance line, homogeneous, and time independent. With the measured electron number density, LTE conditions could be expected for energy levels up to around 12 eV, which just includes the upper level of the Hα transition. Radiation trapping that occurs for the high opacity of the resonance lines may contribute to keeping the shocked gas in LTE. Although the electron number density is not large enough to satisfy relation (1) for the upper state of the NeI 6402-Å transition ($3p[2\frac{1}{2}]_3$) at 18.6 eV, the measured neon temperature agrees with the Hα temperature.

D. Boundary layers

The heated gas behind the shock front was considered to be homogeneous during the LTE plateau when the measurements were made. An indication that the boundary layers are thin can be obtained by comparing the brightness-emissivity temperature for a transition involving the ground state with the temperature determined from a transition that does not involve the ground state. If a cool boundary layer is present, the ground-state transition will result in a value of the emissivity that is too large, because of the lack of emission in the boundary layer. Consequently, the apparent temperature from the ground-state transition will be lower than the temperature derived from a transition that involves only levels that are well above ground and are not populated in the boundary layer.

As boundary layers might have been a problem in our measurements, temperature measurements were made with different elements on a great number of transitions having their energy levels spread from the ground level up to 18.6 eV. The same temperature within the experimental error limits was measured with the FeI ground-level transition (λ3859 Å), as with the excited-level transitions in FeI, OI, HI, and NeI for shocks of the same conditions. The Fe was introduced as a 0.01% admixture of $Fe(CO)_5$. The agreement among the measurements, especially for transitions out of both the ground and excited states, is a strong indication that boundary layers were negligibly thin.

E. Visible spectrum

In order to check whether hydrogen from the shock-tube driver section reached the test region during the measurements, shocks were fired with oxygen replacing hydrogen in the test-gas mixture. From the visible spectrum, no detectable hydrogen was found during the period of the measurements either as an impurity or from the driver gas. Taking into account the transition probabilities of the HI Balmer lines and the OI lines at 7772 Å, we concluded that the density of any hydrogen impurity was at least two orders of magnitude lower than the densities required for the measurements of the HI photoionization cross section. This amount of hydrogen impurity would not affect significantly our HI photoionization cross section measurements or those of CI, NI, and OI.

IV. RESULTS AND DISCUSSION

A. Methods of analysis

Atomic hydrogen was the dominant photoabsorber in the shock-heated hydrogen and neon gas mixture for wavelengths between 911 and 609 Å. Neon absorption was measured to be negligible except for wavelengths near the NeI resonance lines. Rayleigh scattering (see Sec. IV B) by neon is also expected to be negligibly small for all wavelengths used. Our chemical equilibrium calculations show that the density of H_2 is six

orders of magnitude lower than that of HI. We do not see any spectral lines of H_2.

Therefore the atomic photoionization cross section of HI could be derived from the usual expression,

$$\sigma_\lambda = -(1/nl)\ln(I_\lambda/I_{0\lambda}). \quad (2)$$

The number density of atomic hydrogen in the ground level, n, was determined by a chemical equilibrium calculation. The column length l was taken as equal to the shock-tube diagonal; the effect of boundary layers was neglected, since it was believed to be small. The rato between the transmitted intensity I_λ and the incident intensity $I_{0\lambda}$ was determined photographically.

The parameters of each shock-heated gas that was used in the HI photoionization cross-section determination are given in Table I (shock Nos. 1–5). These shocks were selected from a total of nine shocks on the basis that the five had a full set of diagnostic measurements. We found that it was possible to obtain a full set of diagnostics only for shocks of approximately the experimental conditions of these five shocks. For example, the NeI shock emission was not observed at lower temperatures. Shock No. 6 (also described in Table I) did not have a NeI temperature measurement and was excluded from the final data. However, the data analysis for this and the other shocks with incomplete diagnostics yielded HI photoionization curves that fell within the 20% error limits (discussed in Sec. IV C). We concluded that the reliability of our techniques does not depend strongly on the particular shock-tube conditions used.

The shock Mach numbers were about 8. The measured pressure was 5–8% higher than the pressure derived from the measured Mach number and the Rankine-Hutiniot equation. Bengtson *et al.*[26] found a similar discrepancy. The measured temperatures were lower by about 10–20% than those derived from the Rankine-Huginiot ideal-gas equation. This discrepancy is to be exexpected for a mixture of hydrogen and neon.

During the LTE plateau (see Sec. III A) we assume chemical equilibrium exists and that the measured temperature describes the velocity distribution of atoms and ions, the distribution among bound states, and the distribution among ionization stages. The number densities of the atoms, ions, molecules, and electrons that comprise the shock-heated gas were derived from the known initial concentrations and the measured temperature and pressure with a chemical equilibrium computer code. This iterating program uses the Saha equation, the ideal-gas relation, and the charge-neutrality relation. The partition functions used in the program were taken from Drawin and Felenbok,[27] and other parameters such as ionization potentials, dissociation energies, and molecular constants were taken from various reliable sources.[28-30]

Our assumption of LTE is based on the agreement between the excitation temperatures of Hα and the 6402.25-Å NeI line (see Sec. III B), the fact that the measured shock emission intensity is nearly constant during the LTE plateau, and the agreement between the measured electron density and the value determined from the chemical equilibrium calculation (see Sec. III C).

Figure 7 shows an example of the photographic density of the Kodak 101-01 films that were used to measure the photoabsorption spectrum of the shock-heated gas. The six curves represent the following: exposure of the background continuum through an evacuated shock tube, three exposures

TABLE I. Parameters of shock-heated gases.

Parameter	Shock No. 1	2	3	4	5	6	Uncertainty
H in Ne (%)	1.52	1.51	2.03	2.01	2.02	0.72	±1%
Temperature (K)	12 300	12 300	12 200	12 200	12 600	10 600	±2%
Pressure (Torr)	2700	2600	2600	3100	2500	3300	±4%
n_{Ne} (10^{18} cm^{-3})	2.0	2.0	2.0	2.4	1.9	3.0	±5%
n_H (10^{16} cm^{-3})	2.1	2.2	2.9	3.0	2.5	1.8	±5%
n_{Ne^+} (10^{15} cm^{-3})	5.9	5.8	4.6	4.9	.7.1	1.12	
n_{H^+} (10^{16} cm^{-3})	1.02	1.00	1.20	1.33	1.33	0.35	±5%
n_e (10^{16} cm^{-3})	1.61	1.58	1.67	1.82	2.04	0.46	±5%
n_{H_2} (10^{10} cm^{-3})	2	2	4	6	2	2	

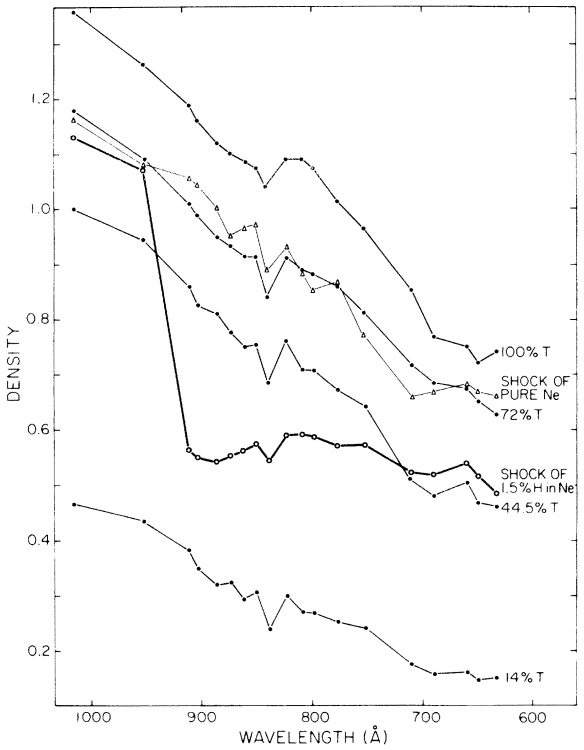

FIG. 7. Measured film densities for photographic exposures of the absorption spectrum of a shock-heated H and Ne gas mixture, and a similar exposure for shock-heated pure neon. The densities for four calibration exposures are also shown. The lines are drawn between the experimental points to aid the eye.

of the continuum from the lamp attenuated by mesh filters of known transmissions, an exposure for transmission through shock-heated pure neon, and an exposure for transmission through a typical hot hydrogen and neon gas mixture. The shock in pure neon did not reach LTE conditions at the time of exposure because the electron number density was too low. The densities follow the intensity variation of the background flashlamp. The wavelengths have been carefully chosen to be in regions with a structure-free continuum in order to avoid measurements near the absorption lines where the flashlamp intensity varies from flash to flash.

The intensity in the observed wavelength region longer than the photoionization threshold was always somewhat lower when the lamp was flashed through the shock-heated gas than when the lamp was flashed through the evacuated shock tube. This effect could be due to misalignment caused by vibrations of the system produced when the squib was fired or to a difference between the flashlamp condition with and without a shock. This effect was seen both for shocks in pure Ne and for those containing hydrogen. The density curves for the shock exposures were therefore normalized for all wavelengths by a constant factor which was determined by comparing the exposure for transmission through the evacuated shock tube to the shock exposure for several wavelengths in the wavelength region well above 920 A.

B. Results

The measured values are collected in Fig. 8, where the absolute photoionization cross section of atomic hydrogen (in Mb) is plotted versus wavelength. The observed data points for five different shocks are plotted for 17 different wavelengths, and the average values of each wavelength are also marked. The curve represents the theoretical values and the dotted lines mark ±20% excursions from the theoretical curve. Almost all observations are within 20%; the average points are in closer agreement with theory and fall within the expected experimental uncertainties (see Sec. IV C). The observed average values are given in Table II, together with the theoretical values that were calculated from the theoretical expression given by Ditchburn and Öpik[31] and the Gaunt factors tabulated by Karzas and Latter.[32]

Our data show a small tendency to be systematically higher than the theoretical values for wavelengths shorter than about 750 Å. Because additional photon loss could be due to Rayleigh scattering from the many Ne atoms, the cross section for this scattering was calculated.[33] The semiempirical calculations used the available data for the ground-state f values[34,35] and for the continuum photoionization cross section[36] of Ne I, and expressions similar to those given in Refs. 37 and 38. However, the calculated cross section for Rayleigh scattering was found to change our measured cross section by only about 1% for $\lambda < 750$ Å.

There is also a very small tendency towards a systematic discrepancy between our measurements and theory for wavelengths around 850 Å. This region corresponds in wavelength to the location of the hydrogen atom-atom radiative recombination continuum. The extreme-shock emission has been found to give a weak continuum for $\lambda \lesssim 915$ Å, which could be measured only with much wider spectrograph slits than were used for the absorption measurements. The measured emission around λ850 Å was found to be larger than that at higher and lower wavelengths. From a limited amount of data it appears likely that the shock emission would explain the systematic

discrepancy around λ850 Å between our measurements and theory. No compensation for these absorption and emission effects has been made in the presented results.

The experimental data points of Beynon and Cairns[11] and of Beynon[12] are also given in Fig. 8. The latter measurements are substantially lower than the present results.

It is sometimes customary to compare the photoionization cross section per atom of diatomic molecules to the photoionization cross section of the constituent atoms. In the case of hydrogen, there is a large difference between the measured molecular cross section per atom of Cook and Metzger[39] and the atomic cross section. This difference is not surprising for the wavelengths of this work or even much shorter wavelengths, because both electrons of H_2 are envolved in the molecular bond.[40]

C. Errors

To establish the expected accuracy of the HI photoionization cross-section measurements, we have estimated the uncertainties in the transmission I/I_0 of the shock-heated gases and the uncertainty in the product nl. The errors in the individual quantities were related to the errors in the cross section σ, using Eq. (2). Uncertainties are given for several representative wavelengths, because the uncertainty in σ depends on the magnitude of I/I_0, which increased with decreasing wavelength.

For each film, a plot of film density D versus the logarithm transmission of the calibration mesh filters was determined for the wavelength of each data point of Fig. 8. A measurement of D at a wavelength of interest for a shock absorption exposure was used to determine the transmission of the shock-heated gas through a comparison to the appropriate calibration curve. For a constant-intensity light source, a comparison at one value of density is sufficient to determine I/I_0. An alternate method that requires two comparisons, one for I and another for I_0, introduces additional uncertainties. The uncertainty in transmission that corresponds to a given uncertainty in film density can be determined from the expression $D=\gamma\log(I/I_0)+C$, an evaluation of the slope of the calibration curve γ, and an evaluation of C, the film density for 100% transmission. Our uncertainties in values of D result from a ±2% uncertainty in interpolating between calibration points, an estimated ±2% nonuniformity across the film, a ±0.5% error in the mesh filter calibration, and the uncertainty in the film calibration curve owing to the ±5% uncertainty in the reproducibility of the flashlamp. For our area of interrogration on the film of 2×10^{-3} cm^2 and film densities ≥ 0.5, we expect an uncertainty in D owing to grainularity of ±0.3%.[41] The values of the photometric errors given here were estimated by comparing several exposures on one film of single flashes of the lamp. Assuming independent errors, the photometric uncertainties in the apparent transmission are ±6%, ±5%, ±6%, and ±6% for wavelengths of 900, 800, 700, and 610 Å, respectively.

Because the intensity of the flashlamp was lower for the conditions during a shock compared to the intensity through the evacuated shock tube (see Sec. IV A), a correction factor was applied to the apparent transmission of the shock-heated gas. At least ten measurements of the correction factor were made, with uncertainties in each

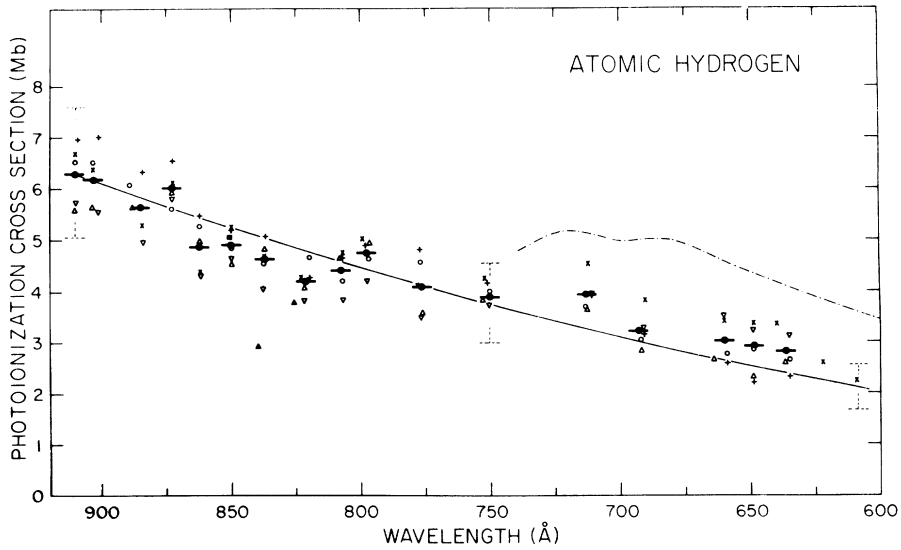

FIG. 8. Photoionization cross section of atomic hydrogen measured for five different shocks (△, ▽, ○, ×, and +), the average of the measurements (solid circle with bar), and the theoretical curve (solid line). Excursions of ± 20% from the theoretical values are indicated at three different wavelengths (dashed line). The experimental data points of Beynon and Cairns (■) and of Beynon (▲) are also shown. The molecular photoionization cross section per atom is indicated by the dot-dash line.

TABLE II. Comparison of measurements and theory.

λ (Å)	$\sigma_{expt.}$ (Mb)	σ_{theor} (Mb)	$\sigma_{expt.}-\sigma_{theor}$ (Mb)	Standard error from theory (%)
911.753	(6.28) [a]	6.31	−(0.03)	(<1)
910	6.25	6.28	−0.03	<1
903	6.16	2.15	0.01	<1
885	5.62	5.83	−0.21	−4
872	5.98	5.61	0.37	7
862	4.85	5.44	−0.59	−11
850	4.83	5.24	−0.41	−8
838	4.60	5.05	−0.45	−9
822	4.19	4.79	−0.60	−13
808	4.40	4.58	−0.18	−4
798	4.73	4.42	0.31	7
777	4.09	4.12	−0.03	−1
752	3.89	3.79	0.10	3
712	3.93	3.25	0.68	21
691	3.22	3.00	0.22	7
660	2.99	2.64	0.35	13
649	2.82	2.53	0.29	11
636	2.81	2.39	0.42	18
623	2.57	2.25	0.32	14
609	2.23	2.12	0.11	5
Average			0.03	

[a] Extrapolated value.

measurement of about ±13% and an uncertainty in the mean of about ±4%. There was also a ±5% uncertainty owing to fluctuations in the shape of the lamp intensity curve. Our estimate of these fluctuations was determined from density-versus-wavelength plots for a shock in pure neon compared to a calibration exposure such as the 72% transmission exposure of Fig. 7. Assuming independent errors, the most probable errors in I/I_0 are ±9%, ±8%, ±9%, and ±9% for 900, 800, 700, and 610 Å, respectively.

There is substantial evidence that the shock-heated gas behind the reflected shock front during the temperature and pressure plateau was in a state of LTE. The uncertainty in the atomic hydrogen number density determination was due mainly to the errors in the temperature measurement, the pressure measurement, and the error in the initial gas mixture concentrations. The accuracy of the brigthness emissivity temperature measurements were limited by the accuracy of the absolute standards, the uncertainty in the absolute current measurements using oscilloscopes and precision resistors, and the presence of boundary layers. We estimate an uncertainty of ±2% in the average value of temperature determined from two measurements for each shock. This estimate compares favorably with the error analyses of others for the brightness emissivity method.[42,43] Further confidence in our estimated accuracy of the temperature measurements stems from the 2% agreement in the two measurements for each shock (see Sec. III B). We estimate a 4% uncertainty in our measurements of pressure. The accuracy of the calibrations of piezoelectric pressure transducers as supplied by the manufacturer is well established.[26,44] The uncertainty in the initial gas mixture concentrations, taking into account the accuracy of the pressure gauges, is about ±1%. From these errors and from the fact that the electron number density calculated with the chemical equilibrium program agreed to within 5% with the measured electron number density, we estimate a most probable error in the hydrogen number density determination of about ±5%.

Using Eq. (2) and assuming independent errors, we find a most probable error in the H I photoionization cross section for the data of each shock of ±8%, ±10%, ±13%, and ±20% for measurements near the wavelengths of 900, 800, 700, and 610 Å, respectively. The dependence on wavelength is due to a systematic tendency to have more absorption for the longer wavelengths. The random errors for the average data points of the five shocks would be reduced by a factor of 0.45.

In addition to the above errors, there were systematic errors. The errors in σ owing to the gas flow out of the openings in the shock tube should be less than +4% (see Sec. II B) and those owing to boundary layers less than +2%. These two effects are to some extent compensated by the observed shock emission. The effect of this was found to vary with wavelengths from about −5% at the series limit to a maximum of about −10% at 850 Å, followed by a rapid decrease with wavelength, becoming smaller than −2% at 800 Å. No compensation for these absorption and emission effects has been made to the results presented here.

An overall estimate was made of the uncertainties in the average absolute determinations of the cross section. These are about ±8% for wavelengths near the series limit, +6% to −15% from about λ850 down to about 800 Å, and then, for shorter wavelengths, +14% to −9%. Treating the theoretical curve as a standard, we give the percent standard error in Table II. Most of the measured average values for $\lambda > 712$ Å fall within the expected uncertainty limits. However, the values for $\lambda < 712$ Å have somewhat larger discrepancies than the most probable errors given here. A possible explanation is that the errors have not accumulated in the most probable way. For

example, if the random sign uncertainties of the individual shocks accumulate to give a +15% error in the mean, that error and the systematic errors would give a possible +21% error in σ. This would account for the difference between theory and experiment. Another possible explanation is that the calculations of Rayleigh scattering are imprecise and that the additional reduction in transmission is due to Rayleigh scattering.

V. SUMMARY

Our newly constructed shock-tube for the extreme ultraviolet has been used to measure absolutely the photoionization cross section of atomic hydrogen. The agreement between the observed and the theoretical values demonstrates the capability of the apparatus described in this paper for making absolute photoabsorption measurements with uncertainties in the ±(7–20)% range. Our program to measure the absolute photoionization cross sections of OI, CI, and NI will continue after some further improvements of the apparatus.

ACKNOWLEDGMENTS

The authors wish to express their sincere gratitude to Dr. W. H. Wurster for descriptions of his apparatus and related discussions. We are indebted to Dr. G. A. Victor for his calculations of the Rayleigh scattering cross section. We wish to thank J. Caunt and J. Crawford for engineering assistance with the design of the shock tube and J. Crawford in particular for his unusual design of the shock absorbers. We also thank W. Menzi and W. E. Millikin, Jr., for their technical assistance. This work was supported by the National Aeronautics and Space Administration under grant NGL 22-007-006.

[1]J. E. Vernazza, E. H. Avrett, and R. Loeser, Astrophys. J. 184, 605 (1973).
[2]P. M. Banks and G. Kockarts, *Aeronomy*, Parts A and B (Academic, New York, 1973).
[3]J. C. G. Walker, D. G. Torr, P. B. Hays, D. W. Rusch, K. Docken, G. Victor, and M. Oppenheimer, J. Geophys. Res. 80, 1026 (1975).
[4]J. L. Kohl and W. H. Parkinson, Astrophys. J. 184, 641 (1973).
[5]J. L. Carlsten and T. J. McIlrath, J. Phys. B 6, L284 (1973).
[6]T, J. McIlrath and R. J. Sandeman, J. Phys. B 5, L217 (1972).
[7]J. C. Rich, Astrophys. J. 148, 275 (1967).
[8]M. C. E. Huber, R. J. Sandeman, and E. F. Tubbs, Proc. R. Soc. A 342, 431 (1975).
[9]Y. Suguira, J. Phys. Radium 8, 113 (1927).
[10]H. A. Bethe and E. E. Salpeter, *Quantum Mechanics of One- and Two-Electron Systems* (Academic, New York, 1957).
[11]J. D. E. Beynon and R. B. Cairns, Proc. Phys. Soc. Lond. 86, 1343 (1965).
[12]J. D. E. Beynon, Proc. Phys. Soc. Lond. 89, 59 (1966).
[13]P. V. Marrone and W. H. Wurster, J. Quant. Spectrosc. Radiat. Transfer 11, 327 (1971).
[14]S. Dushman, in *Scientific Foundations of Vacuum Technique*, edited by J. M. Lafferty, 2nd ed. (Wiley, New York, 1962).
[15]D. J. Santeler, D. W. Jones, D. H. Holkeboer, and F. Pazano, *Vacuum Technology and Space Simulation*, NASA SP-105 (NASA, U. S. GPO, Washington, D. C., 1967).
[16]J. E. G. Wheaton, Appl. Opt. 3, 1247 (1964).
[17]W. H. Parkinson and E. M. Reeves, Proc. R. Soc. A 282, 265 (1964).
[18]M. C. E. Huber and W. H. Parkinson, Astrophys. J. 172, 229 (1972).
[19]G. L. Grasdaleu, M. C. E. Huber, and G. H. Newsom, Rev. Sci. Instrum. 39, 886 (1968).
[20]A. G. Gaydon and I. R. Hurle, *The Shock Tube in High-Temperature Chemical Physics* (Reinhold, New York, 1963), pp. 9–28.
[21]W. R. S. Garton, W. H. Parkinson, and E. M. Reeves, Proc. Phys. Soc. Lond. 88, 771 (1966).
[22]W. Lochte-Holtgreven, in *Plasma Diagnostics*, edited by W. Lochte-Holtgreven (North-Holland, Amsterdam, and Wiley, New York, 1968), pp. 135–249.
[23]P. Kepple and H. R. Griem, Phys. Rev. 173, 317 (1968).
[24]H. R. Griem, *Plasma Spectroscopy* (McGraw-Hill, New York, 1964).
[25]H. R. Griem, Phys. Rev. 131, 1170 (1963).
[26]R. D. Bengtson, M. H. Miller, D. W. Koopman, and T. D. Wilkerson, Phys. Fluids 13, 372 (1970).
[27]H. W. Drawin and P. Felenbok, *Data for Plasmas in Local Thermodynamic Equilibrium* (Gauthier-Villars, Paris, 1965).
[28]G. Herzberg, *Spectra of Diatomic Molecules* (Van Nostrand, Princeton, 1950).
[29]B. Rosen, *International Tables of Selected Constants 17, Spectroscopic Data Relative to Diatomic Molecules* (Pergamon, New York, 1970).
[30]C. E. Moore, *Atomic Energy Levels*, Natl. Bur. Stand. Circ. No. 467, Vol. 1 (U. S. GPO, Washington, D. C., 1949).
[31]R. W. Ditchburn and U. Öpik, in *Atomic and Molecular Processes*, edited by D. R. Bates (Academic, New York, 1962), p. 79.
[32]W. J. Karzas and R. Latter, Astrophys. J. Suppl. Ser. 6, 167 (1961).
[33]G. Victor (personal communication).
[34]R. F. Stewart, Mol. Phys. 30, 1283 (1975).
[35]G. M. Lawrence and H. S. Liszt, Phys. Rev. 178, 122 (1969).
[36]R. D. Hudson and L. J. Kieffer, At. Data 2, 205 (1971),

with references on Ne I.
[37]Y. M. Chan and A. Dalgarno, Proc. Phys. Soc. Lond. 85, 227 (1965) [Eqs. (1) and (16)].
[38]A. Dalgarno and A. E. Kingston, Proc. R. Soc. A 259, 424 (1960) [Eq. (1)].
[39]G. R. Cook and P. H. Metzger, J. Opt. Soc. Am. 54, 968 (1964).
[40]J. W. Cooper, Phys. Rev. A 9, 2236 (1974).
[41]W. M. Burton, A. T. Hatter, and A. Ridgeley, Appl. Opt. 12, 1851 (1973).
[42]M. H. Miller, R. A. Roig, and R. D. Bengtson, Phys. Rev. A 4, 1709 (1971).
[43]J. Allen, Ph. D. thesis (Harvard University, 1973) (unpublished).
[44]M. Eckart, Ph. D. thesis (Harvard University, 1974) (unpublished).

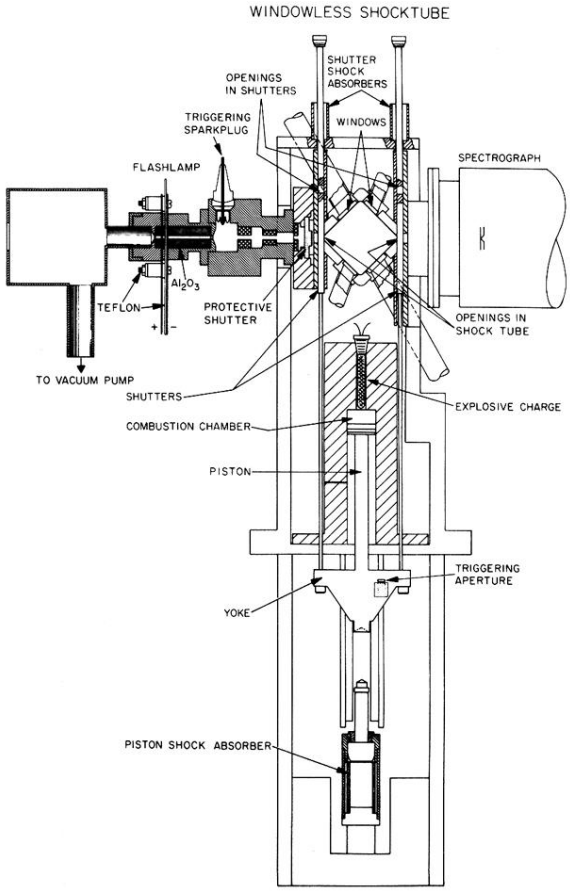

FIG. 2. Cross-sectional view of the shock tube showing the shutter mechanism and the flashlamp.

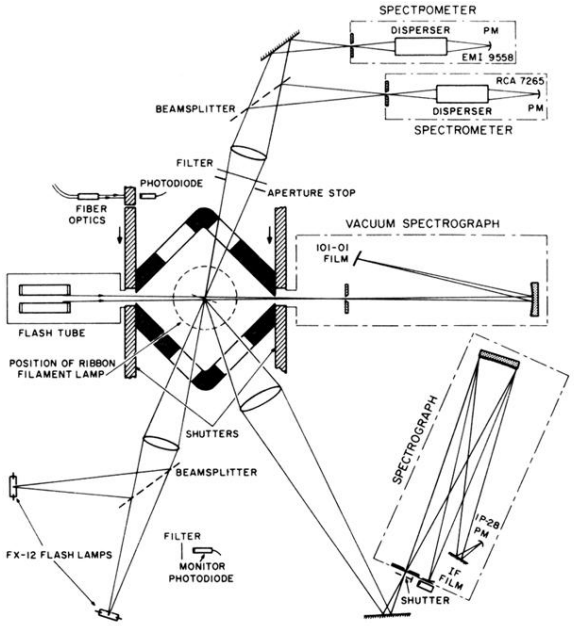

FIG. 3. Schematic diagram of the optical arrangements for the absorption measurements, the brightness-emissitivy temperature measurements, and the determination of the visible spectrum.